ELSEVIER

Biophysical Chemistry 85 (2000) 199–208

Biophysical Chemistry

www.elsevier.nl/locate/bpc

The phases of small networks of chemical reactors and neurons

N. Schinor, F.W. Schneider*

Institute of Physical Chemistry, University of Wuerzburg, Am Hubland, 97074 Wuerzburg, Germany

Received 12 October 1999; received in revised form 9 December 1999; accepted 9 December 1999

Abstract

We present an experimental study of the phase relationships observed in small reactor networks consisting of two and three continuous flow stirred tank reactors. In the three-reactor network one chemical oscillator is coupled to two other reactors in parallel in analogy to a small neural net. Each reactor contains an identical reaction mixture of the excitable Belousov–Zhabotinsky reaction which is characterized by its bifurcation diagram, where the electrical current is the bifurcation parameter. Coupling between the reactors is electrical via Pt-working electrodes and it can be either repulsive (inhibitory) or attractive (excitatory). An external electrical stimulus is applied to all three reactors in the form of an asymmetric electrical current pulse which sweeps across the bifurcation diagram. As a consequence, all three reactors oscillate with characteristic oscillation patterns or remain silent in analogy to the firing of neurons. The observed phase behavior depends on the type of coupling in a complex way. This situation is analogous to the in vivo measurements on single neurons (local neurons and projection neurons) performed by G. Laurent and co-workers on the olfactory system of the locust. We propose a simple neural network similar to the reactor network using the Hodgkin–Huxley model to simulate the action potentials of the coupled single neurons. Analogies between the reactor network and the neural network are discussed.

Keywords: Non-linear dynamics; Reactor and neural networks; Action potentials of single neurons; Phase relations; Computer simulations

* Corresponding author. Tel.: +49-931-8886-300; fax: +49-931-888-6302.
E-mail address: fws@phys-chemie.uni-wruerzburg.de (F.W. Schneider).

0301-4622/00/$ - see front matter
PII: S0301-4622(99)00155-6

1. Introduction

We have been particularly interested in small networks of chemical reactors that are capable of learning and recognizing dynamical reactor patterns [1–4]. These studies may serve to better understand relevant principles in biological systems. The individual reactors are coupled in specific ways. We prefer the method of electrical coupling through Pt-working electrodes because it is direct and relatively fast and it can be either excitatory or inhibitory whereas mass transfer coupling can only be excitatory and slow. Furthermore, electrical coupling is closer to (but not identical with) the coupling of neurons in in vivo systems. In this work we present small reactor networks consisting of two and three continuous flow stirred tank reactors (CSTRs) that contain an identical reaction mixture of the excitable Belousov–Zhabotinsky (BZ) reaction although any other suitable chemical oscillators would do as well. The reactors are coupled via electrical currents that cause redox processes at the Pt-working electrodes which perturb the chemical BZ reaction and can cause transitions between the oscillatory and the steady states of the reaction according to the bifurcation scenario. The central issue is the study of the complex phase behavior (coherence and incoherence) of the coupled reactors as a consequence of the nature and strength of electrical coupling between them.

Previous work provided the basis of the present study. In our first experiments [1] we prepared a focal steady state in each of four electrically coupled BZ reactors. An external sinusoidal perturbation by an electrical current provided global coupling of the reactors leading to the recognition of one of two stored phase patterns with a 50% probability. In a second study, all four BZ reactors were placed in their oscillatory states [2]. Global coupling by external rectangular pulses of the electrical current lead to a 1:2 response of the oscillation period, which enabled a unique recognition of either of two encodable phase patterns. In a third study [3] we employed local instead of global coupling between four reactors according to a Hopfield net. Each of the four reactors was placed either in an oscillatory or in a nodal excitable steady state depending on the magnitude of the applied electrical current. We introduced an averaging procedure of the oscillatory signal in order to implement inhibitory coupling as well. Excitatory as well as inhibitory coupling are necessary to achieve a unique recognition of all presented patterns.

In an extended study we employed a larger network of eight reactors which allowed an improved recognition process by encoding three reactor patterns instead of two [4]. As a result, the reactor network also successfully associated the presented (initial) patterns with one of the three encoded patterns to which it had the least number of errors in a very robust and rapid way.

In further work on electrically coupled oscillators [5] we studied in more detail the actual propagation of action potentials (spikes) in 3–6 chemical reactors that were coupled in a linear and in a cyclic network starting with an excitable steady state in each reactor. In the cyclic net, self-sustaining traveling waves of oscillatory spikes were measured for the first time. The phase behavior of mutually coupled chemical reactors was also studied in networks of two, three and four mutually coupled reactors in their oscillatory initial states [5]. When the reactors were mutually coupled through attractive interactions in both directions, in-phase coherence of all oscillating reactors was observed, whereas out-of-phase motion occurred for repulsive coupling which was stable only when the reactor network was sufficiently small (≤ 3).

In the following we present a phenomenological study of the phase behavior of two and three chemical reactors, where the latter are coupled in a similar fashion as in a simple neural net. We propose a simple neural network which provides a phenomenological explanation of the impressive experiments by Laurent and co-workers [6–9] of the action potentials of single neurons in the olfactory system of the locust and in the bee.

2. Experimental

Three identical CSTRs (4.2 ml) are constructed from plexiglas and each contains a Pt-working

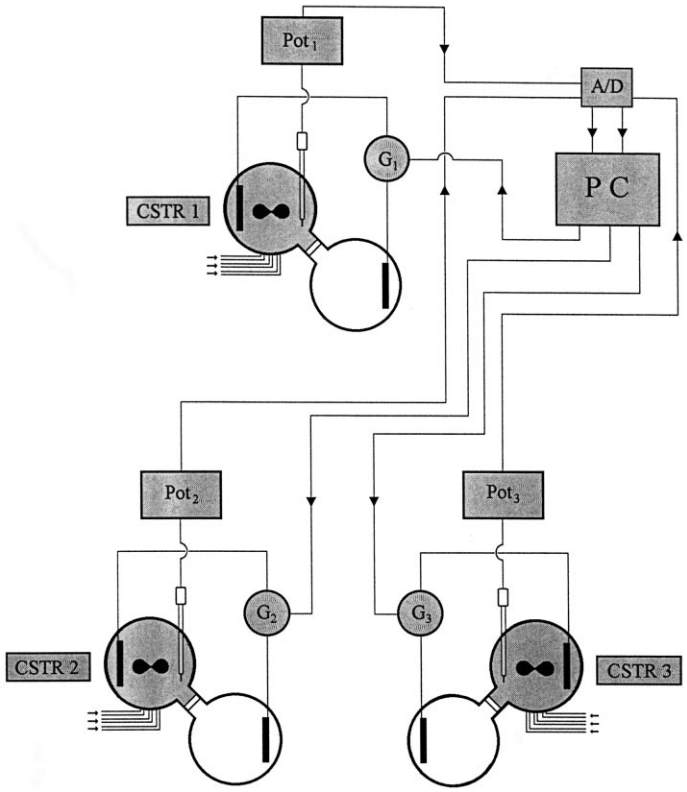

Fig. 1. Three-reactor network: each CSTR contains a Pt-working electrode, a monitoring Pt|AG|AgCl redox electrode and a magnetic stirrer. Each CSTR is connected to its own reference compartment which is separated by a porous teflon membrane, Pot_i are redox potentials as monitored by the Pt|Ag|AgCl electrode, G_i are the electric currents applied to the Pt-working electrodes by galvanostats; A/D, analogue to digital converter; electrical coupling is calculated according to Eq. (2) by a personal computer.

electrode (~ 2.0 cm^2), a monitoring Pt|Ag|AgCl redox electrode and a magnetic stirrer (600 rev./min) (Fig. 1). Each CSTR has its own reference half cell which is separated by a teflon membrane. The reference half cell also contains a Pt-working electrode and a sulfuric acid solution (0.4 mol/l). The reactants enter through the bottom of each CSTR and the contents flows out at the top. Three reactant streams are fed by a syringe pump with three syringes: Syringe I, $NaBrO_3$ (0.42 mol/l); syringe II, $Ce_2(SO_4)_3$ (1.5×10^{-3} mol/l), malonic acid (0.9 mol/l), and syringe III, sulfuric acid (1.12 mol/l).

The redox potentials ('action potentials') of the monitoring electrodes are digitally recorded (1 Hz) and presented in arbitrary units due to unavoidable variations in their sensitivities. Electrical currents G_i are continuously calculated by a PC according to Eqs. (1) and (2) and they are delivered to the Pt-working electrodes in each CSTR through galvanostats (E&G Instruments). The working electrodes may be run either as anodes or as cathodes.

2.1. Flow rate, electric current and bifurcation diagram

A fixed flow rate is chosen at which each reactor oscillates in a well-known way [2–5] in the absence of an electric current. The feed concentrations and the flow rates are identical in each reactor ($k_f = 6.0 \times 10^{-4}$ s^{-1}) corresponding to an average residence time of 27.8 min.

When a weak (positive) cathodic current is

applied to an uncoupled single reactor in the free-running oscillatory mode of the BZ reaction, the oscillations change into a nodal steady state at 0.85 mA [2–5]. This point is termed a SNIPER (saddle node infinite period) bifurcation at which a limit cycle collides with a saddle node leading to an oscillation of infinite period. In addition, we observed an anodic SNIPER bifurcation which occurs at −0.25 mA when the current is reversed at the Pt-working electrode for the present concentrations and flow rate. This situation may be summarized in a bifurcation diagram (Fig. 2) which shows that the amplitudes of the oscillations abruptly disappear at the two SNIPER points while the oscillation frequencies decline to zero (= infinite period) in a more gradual way for both cathodic and anodic currents.

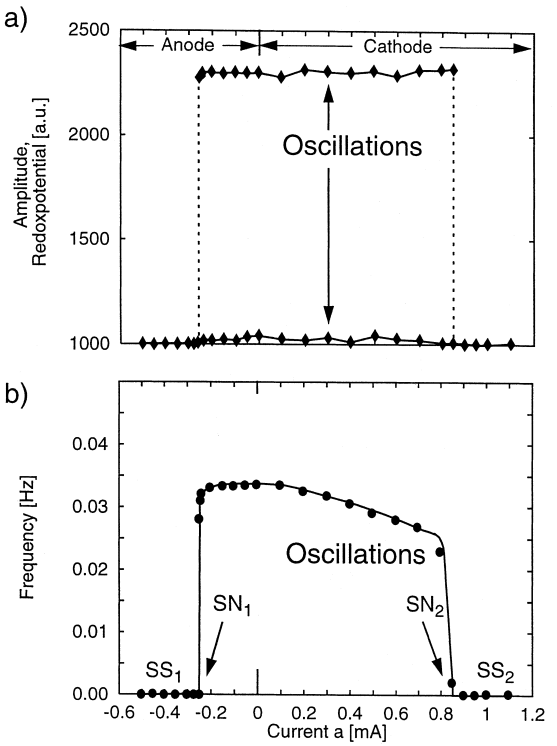

Fig. 2. (a) Experimental bifurcation diagram for the given BZ concentrations (see text) at $k_f = 6.0 \times 10^{-4}$ s^{-1}, amplitude (maxima and minima) of the redox potential vs. current a (mA), steady state regions SS_1 and SS_2 with oscillatory region in-between, SNIPER bifurcations SN_1 (−0.25 mA) and SN_2 (0.85 mA), Pt-working electrode as anode for $a < 0$ and as cathode for $a > 0$. The redox potential for the steady state has been arbitrarily set at 1000 arb. units as a reference; the steady states are termed as excitable; (b) Frequency (Hz) vs. current a (mA); the points of infinite period (zero frequency) are SN_1 and SN_2 as in (a).

3. Results and discussion

3.1. Two coupled reactors

When two oscillating BZ reactors (R1 and R2) of similar frequencies are coupled unidirectionally, R1 'drives' R2 according to the coupling equation for G_2:

$$G_1 = \text{bias}_1$$

$$G_2 = \text{bias}_2 + w(\text{Pot}_1 - 1000) \quad (1)$$

where G_1 and G_2 are positive currents delivered to the Pt-working electrodes of each reactor by the galvanostats. The Pt-working electrode is the cathode. Bias_1 and bias_2 are constant positive currents which place the reaction either in the oscillatory region or in a steady state; Pot_1 is the oscillating potential of reactor 1 as measured by the reference electrode. Our chosen reference state is the nodal steady state (SS_2). The potential of this reference state is assigned the value of 1000 arbitrary units. The coupling strength between R1 and R2 is denoted by w; it is either attractive or repulsive with $w < 0$ or $w > 0$ for a cathodic current, respectively, whereas for an anodic current w has the opposite sign, namely $w > 0$ for an attractive and $w < 0$ for a repulsive coupling strength.

3.2. Phase behavior

There are three main regions of coupling which are defined by the bifurcation diagram of the BZ reaction (Fig. 2):

(a) *R1 and R2 oscillate in the region of positive current* of the bifurcation diagram with a negative (attractive) coupling interaction between R1 and

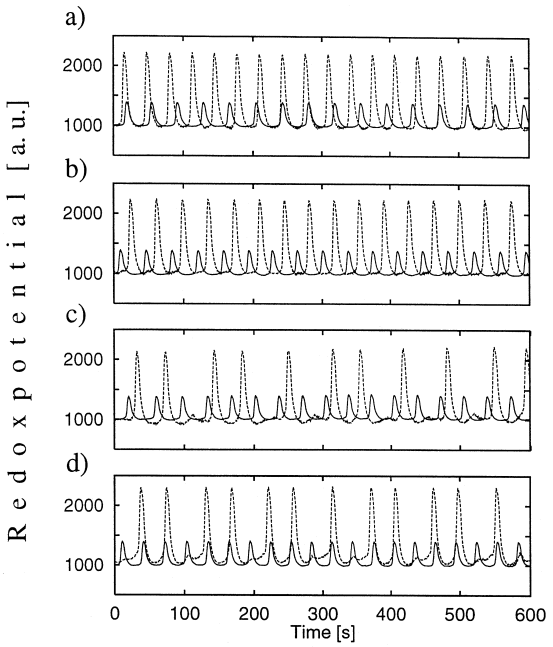

Fig. 3. Unidirectional coupling of two reactors R1 (full line) and R2 (dotted line): (a) Attractive coupling ($w = -0.8$ μA/V), $bias_1$ 700 μA, $bias_2$ 400 μA: phase shift varies periodically. (b) Repulsive coupling ($w = +0.8$ μA/V), $bias_i$ as in (a): out-of-phase oscillations. (c) Oscillations of R1 perturb the steady state SS_2 (of R2) with attractive coupling ($w = -0.8$ μA/V), $bias_1$ 700 μA/V, $bias_2$ 950 μA/V: phase shift between R1 and R2. (d) Oscillations of R1 perturb an oscillatory state of R2 (close to SN_2) with ($w = +0.8$ μA/V), $bias_1$ 700 μA/V, $bias_2$ 750 μA/V: zero phase shift between R1 and R2.

R2. As a result, the phase shift between R1 and R2 is found to vary periodically through all phase angles for the present BZ reaction (Fig. 3a). A positive (repulsive) coupling interaction, however, eventually leads to 180° out-of-phase oscillations (Fig. 3b).

(b) When the periodic output of R1 is allowed to perturb the *steady state* SS_2 (of R2) with a negative coupling interaction, the SNIPER point SN_2 is crossed periodically from the steady state in the direction of the oscillatory region (to the left) and back as w is negative and ($Pot_1 - 1000$) is always positive. This generates a phase shift in R2 relative to R1 whose value depends on the distance of SS_2 from the bifurcation point SN_2. The phase is delayed more strongly when the perturbing Pot_1 is smaller and the initial steady state of R2 is farther away from the bifurcation point SN_2. This situation is similar to the 'time advance coding' concept of Hopfield [10] which we have verified experimentally for a Hopf bifurcation in the minimal-bromate oscillator [11].

(c) Another important case of coupling concerns the transition in the opposite direction to case (b), starting from the *oscillatory* region of R2 to its *steady* state SS_2 (Fig. 3d) where w is positive. This transition shows a zero phase shift between R1 and R2 when the oscillating R2 is close to SN_2. Here R2 is found to fire always within the width of R1.

Since the bifurcation diagram for the BZ reaction is a close mirror image for the cathodic and the anodic current (Fig. 2), the observations in (b) and (c) are also valid for the anodic SNIPER point SN_1, but with opposite signs for w.

3.3. A three-reactor network

Here we investigate a reactor network that consists of three BZ reactors (Fig. 4) where the first reactor (R1) is coupled unidirectionally with the second (R2) and, in parallel, unidirectionally with the third reactor R3; R2 and R3 being mutually *un*coupled. This reactor network has

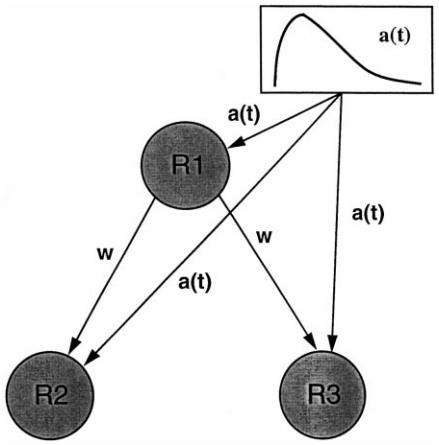

Fig. 4. Three-reactor-network: R1 is coupled unidirectionally to R2 and R3 in parallel with coupling strength w; $a(t)$ is the time-dependent external stimulus which sweeps the BZ reaction across its bifurcation diagram.

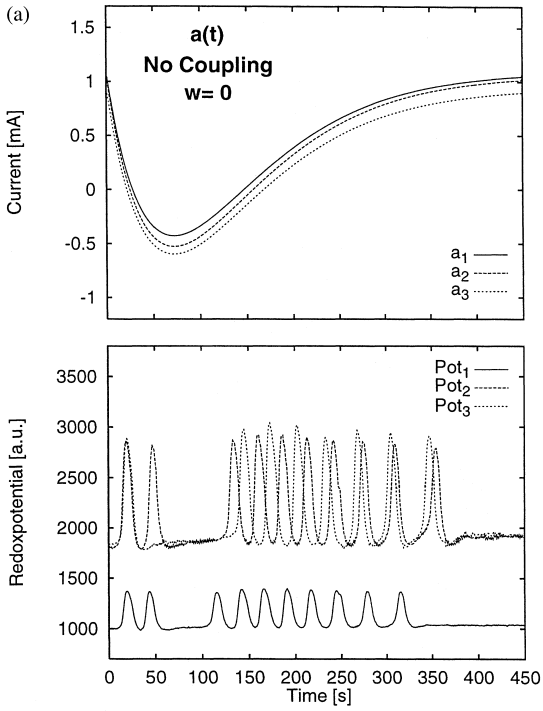

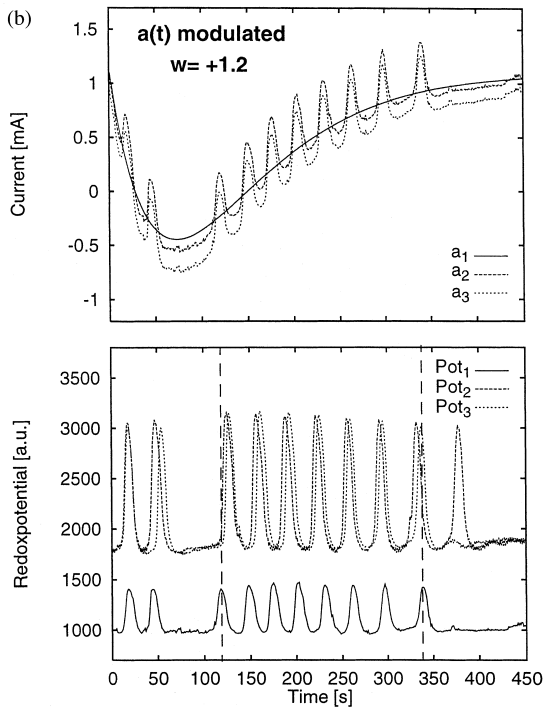

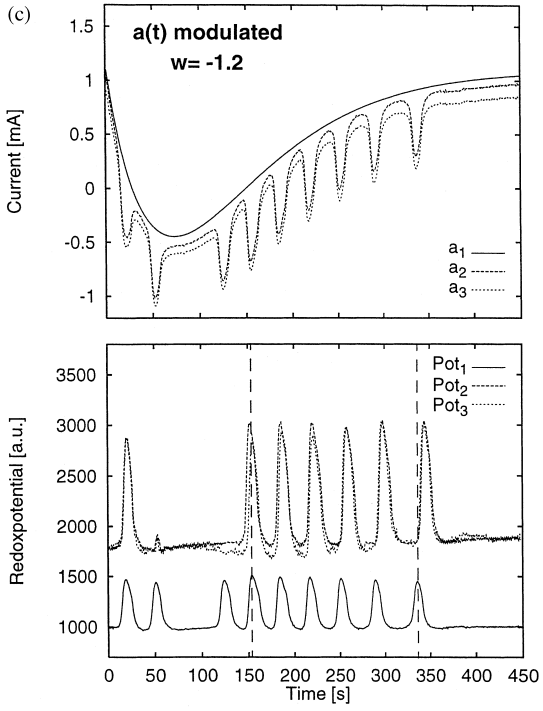

Fig. 5a. Action potentials of the three-reactor network (Fig. 4): (a) All three reactors are uncoupled, $w = 0$, the stimuli are negative with slightly different amplitudes, redox potentials (Pot_i) (signatures) of each reactor vs. time (see text). (b) Positive coupling ($w = +1.2$ μA/V) between R1 and R2 and between R1 and R3; stimuli a_2 and a_3 are modulated by Pot_1 of R1 [Eq. (2)], redox potentials Pot_i vs. time; the perpendicular lines serve as a visual orientation. (c) Negative coupling ($w = -1.2$ μA/V); similar as in (b).

been constructed to generate chemical 'action potentials' when it is stimulated by an external electric current $a(t)$ in analogy to the stimulation of single neurons by an odor in the olfactory system of the locust [6–8] and the honey bee [9].

The coupling equations for the three-reactor network are:

$$G_1 = \mathrm{bias}_1 - a_1(t)$$

$$G_2 = \mathrm{bias}_2 - a_2(t) + w(\mathrm{Pot}_1 - 1000) \qquad (2)$$

$$G_3 = \mathrm{bias}_3 - a_3(t) + w(\mathrm{Pot}_1 - 1000)$$

where the parameters G_i, bias_i, Pot_1 and w are the same as in Eq. (1) except for the addition of the third reactor and a time-dependent stimulus $a_i(t)$. The stimulus $a_i(t)$ is subtracted since the initial state is chosen to be a steady state of high current (SS_2). The values for $a_i(t)$ are slightly different in amplitude for the three reactors due to experimental variations. The important point is to determine the sign and the strength of coupling necessary to shift the phases between the first reactor and the other two reactors in a specific way. The resulting phases of the two mutually *un*coupled reactors R2 and R3 will also be of interest.

3.4. The external stimulus a(t): how to generate action potentials

In order to generate patterns of action potentials, we use an external time dependent electric current $a(t)$. This external stimulus will be swept across the oscillatory region of the bifurcation diagram starting from one of the excitable steady states to the other excitable steady state and back again. The sweeping rate of the electric stimulus determines the signature (oscillatory pattern) of the responding reactors (R2 and R3) in a very sensitive way.

An 'infinite' number of signatures of action potentials may be generated, in principle, as a consequence of the shape and the amplitude of the stimulus depending on the dynamics of the reaction and the rate at which the stimulus is swept across the bifurcation diagram.

In the following experiments the shape of $a(t)$ is characterized by its amplitude and two constants in analogy to the equation for the kinetics of two consecutive reaction steps. We apply similar $a_i(t)$ to all three reactors in order to obtain similar oscillation patterns in the presence of inhibitory or excitatory coupling as well as in the absence of any coupling ($w = 0$). $a(t)$ is equivalent to global coupling.

As a representative result of ~ 60 experiments we show three types of experiments with and without unidirectional coupling between R1 and R2 and between R1 and R3 in Fig. 5. All initial steady states in the reactors are cathodic in our experiments; $a(t)$ is started at SS_2 and swept from the cathodic region (positive current) through zero into the anodic region (negative current) of the oscillations beyond the SNIPER point SN_1 (approx. -0.25 mA) well into the SS_1 region depending on the amplitude of $a(t)$. The return sweep starts in the 'minimum' of $a(t)$ and the stimulus recrosses the oscillatory region back to the starting point SS_2.

In the following we present an interpretation of the complex phases of the action potentials in Fig. 5. It is noted that it is the phase behavior between R1 and R2 (R3) which is significantly affected by the coupling mode [Eq. (2)], whereas any phase difference between R2 and R3 is more affected by the experimental scatter in the SNIPER points. Importantly, the oscillation frequencies are not constant in the oscillatory region (Fig. 2); they decrease to zero at the respective SNIPER points (SN_1 and SN_2) adding a further complexity to the responding action potentials.

3.5. Phase behavior

A complex phase behavior is observed for negative and positive coupling which can be understood on the basis of our phase measurements for undirectional coupling in the two-reactor network [Eq. (1)]. There are three groups of experiments:

(a) All three reactors are uncoupled, i.e. $w = 0$. As a result the individual signatures of all three reactors are similar, because they receive the same external stimulus which is not modulated for $w = 0$ (Fig. 5a).

At the start two superimposed spikes are observed (at ~ 20 s) due to the simultaneous firing of R2 and R3 when $a_1(t)$ and $a_2(t)$ simultaneously cross the bifurcation point SN_2 into the oscillatory region and further into the nodal steady state region of SS_1 where the oscillations disappear (50–120 s). The re-entry of $a(t)$ into the oscillatory region causes R1, R2, and R3 to fire with practically no coherence since the experimental oscillators show slightly different frequen-

cies and the reactors are not coupled. Finally, when $a(t)$ has returned to its initial steady state SS_2, the oscillations in R1, R2 and R3 disappear.

(b) How does the situation change when a positive coupling strength is introduced (between R1 and R2 and between R1 and R3 with $w = 1.2$ $\mu A/V$)? Starting at SS_2, R2 and R3 receive a stimulus $a(t)$ which is modulated by the contribution from the periodic output (Pot_1) of R1 according to Eq. (2). As a result, the first spike at 20 s is identical for R2 and R3 since the sweep rates are fast and identical for R2 and R3 and modulation is not very important at the start. Due to positive modulation both reactors R2 and R3 display second spikes (at ~ 50 s), whose phases are somewhat different. The reason is that the system has already visited its steady state (SS_1) once (at ~ 40 s) after which the modulation has caused a single transition from the SS_1 into the oscillatory region (at ~ 45 s) which is always accompanied by a phase shift between R1 and R2 and between R1 and R3. Furthermore, the SNIPER points SN_1 in R2 and R3 are not exactly identical in the experiment. A gap of spikes occurs (between ~ 50 and 120 s), for the same reason as in Fig. 5a, since all reactors are safely in their steady state region SS_1. The re-entry from SS_1 into the oscillatory region (at $t \sim 120$ s) causes phase shifts between R1 and R2 (R3) due to the 'time advance coding' effect [10,11] as previously mentioned. There is still a phase difference between R2 and R3 (which, in this experiment, happens to remain approximately constant with time), due to a small difference in the SNIPER points.

As the stimulus sweeps towards the SNIPER point SN_2, the positive modulation carries it more rapidly across SN_2 with the result that the phase difference between R1 and R2 (R3) is nearly zero as expected for a transition from an oscillatory to a steady state (see Fig. 3d). The stimulus $a(t)$ returns the system to its initial steady state SS_2 after ~ 350 s except for R2 which fires for a last time at ~ 375 s (Fig. 5b).

(c) The coupling strength is negative, i.e. $w = -1.2$ $\mu A/V$. The stimulus $a(t)$ is applied in a similar fashion as in case (b) but it is modulated in the negative direction of the current (Fig. 5c) according to Eq. (2). As a result, the first spike is again practically identical for R2 and R3, whereas the second spike is missing in both reactors since SS_1 has been further stabilized ('hyperpolarized') by the negative modulation (at ~ 53 s). Therefore a larger gap occurs here ($30 \text{ s} < t < 160$ s) whereas R1 fires as in Fig. 5a,b. After the stimulus has brought the system back into the oscillatory region, the modulation reverts it momentarily into its steady state SS_1. Thus there should be a zero phase shift between R1 and R2 and between R1 and R3 as observed. As the stimulus has returned the system through the entire oscillatory region across the SNIPER point (SN_2) back to its initial steady state SS_2, a negative modulation carries it back momentarily deep into its oscillatory region at $t \sim 330$ s. Thus two spikes (R2 and R3) are generated ($t \sim 350$ s) which are phase shifted relative to R1 as required. The phase shift between R2 and R3 is close to zero in this particular experiment, since the experimental SNIPER points and the frequencies of the two oscillators are nearly identical.

3.6. Comparison between the reactor and neural network

From their impressive in vivo measurements on the olfactory system of the locust and the bee G. Laurent and co-workers reported [6–9] that the coupling between a local neuron (LN) and a projection neuron (PN) is inhibitory, since the firing of a PN follows the firing of a LN with a phase shift (Fig. 6a) during the time of presentation of a stimulus representing an odor (cherry). Another projection neuron shows an action potential measured for the odor of mint (Fig. 6b) which is similar in appearance to the above reactor potential (Fig. 5b). Note that the bifurcation diagram for the BZ reaction (Fig. 2) has been rapidly traversed from the upper steady state (SS_2) through the oscillatory region to the lower steady state (SS_1), where the system stays for some time (~ 70 s) while $a(t)$ passes through its extremum. This has caused an absence of spikes (between ~ 50 s and 120 s) between the two groups of spikes. On the 'slower' return path of $a(t)$ towards SS_2 the system has sufficient time to oscillate for a few oscillations with a frequency,

which decreases according to the bifurcation diagram (Fig. 2). A similar situation may be observed for yet another projection neuron for the odor of cineole (Fig. 6c). When picrotoxin is added to the latter, the local field potential disappears indicating that the coherence between the PN-oscillations is lost although the projection neuron continues to fire with an approximately similar firing pattern as before. Thus picrotoxin has eliminated the inhibitory action of the LN on the PN. This corresponds to a smaller and slower stimulus (not shown) for our reactor network with no interaction ($w = 0$) between R1 and R2 and between R1 and R3, where R2 and R3 will fire incoherently with about the same pattern as with inhibitory coupling. The local field potential in a neuronal system measures the sum of the potentials of many projection neurons [6–9]. When a group of PNs fires synchronously, the LFP is well developed (Fig. 6b,c). If the phases vary with time, the LFP will be relatively small. In analogy to the neuronal LFP one may measure the sum of the redox potentials of the driven reactors (R2 and R3) which will also be large and regular if the responding reactors R2 and R3 fire synchronously (even if they are out-of-phase with the modulating reactor R1). The chemical LFP will be finite but small when the driven reactors show variable phases with time for $w = 0$ (Fig. 5a), since the chemical oscillations are relatively broad and they partially overlap in the sum. Obviously, the frequency of the neuronal action potentials is larger and the reactor potentials are broader than those of the neuronal spikes.

In the reactor net the interpretation of w as excitatory or inhibitory depends on the reference steady state. If w modulates the system away from the excitable steady state into the oscillatory region w is termed as excitatory; if w sweeps the bifurcation parameter into the opposite direction, i.e. from oscillatory to steady state, w is inhibitory. Therefore the response behavior is complex for a modulated pulse of large amplitude, which travels across the whole bifurcation diagram. When the stimulus sweeps the system from one steady state all the way through the oscillatory region into the other, it is always first excitatory relative to the first steady state and inhibitory relative to the second. The same argument applies to the return sweep.

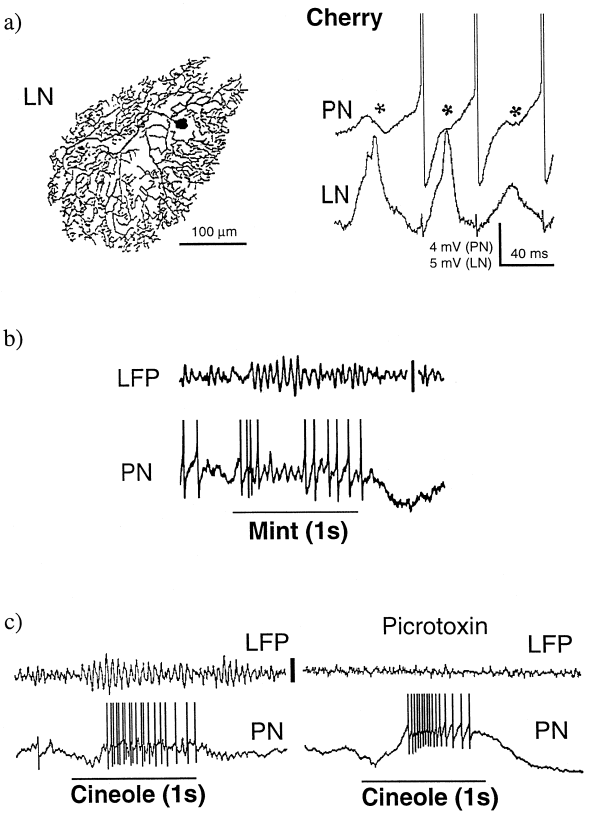

Fig. 6. In vivo recordings [6] from an antennal local neuron (LN) and post-synaptic projection neurons (PNs) during responses to various odors in a locust. PN spikes are clipped. With permission of the authors. (a) Camera lucida drawing of a LN and simultaneous intracellular recordings from a LN and a post-synaptic PN during a response to a cherry odor. (b) Local field potential (LFP) of a group of PNs and intracellular recording of a PN (different from a) for the odor of mint, vertical: 0.5 mV (LFP); 5 mV (PN). (c) LFP and PN (different from a,b) for the odor of cineole without (left) and with (right) 5 mM picrotoxin, vertical: 200 μV (LFP); 10 mV (PN).

4. Conclusions

Our electrical coupling experiments of two unidirectionally coupled chemical oscillators show that their phases vary periodically if the coupling is attractive and the two BZ oscillators are nearly identical. For repulsive coupling 180° out-of-phase

coherence is obtained after several oscillations. These observations provide the basis for understanding the phases of the three-reactor network.

When all three reactors receive identical external stimuli in the form of a long asymmetric pulse, their phases vary with time due to the fact that the three oscillators display slightly different frequencies. Coherence (i.e. the existence of time-invariant phases) between all reactors can be achieved through (electrical) unidirectional coupling when one reactor drives (modulates) the other two reactors in parallel. For this case the two driven reactors become coherent with each other as a consequence of the modulation which they receive from the first reactor owing to coupling. The phase behavior between the modulating reactor and the driven reactors is complex since it depends strongly on the initial state, the sweeping rate of $a(t)$ and on the amplitude of the modulation. Any transition from the steady state of a reactor into its oscillatory region is always accompanied with a phase shift between the driving and the driven reactor. However, modulation in the reverse direction, from the oscillatory to the steady state region, shows a nearly zero phase shift.

The sweeping rate and amplitude of an applied external stimulus ('odor') determines the appearance of the oscillatory (firing) patterns of the responding reactors. The firing patterns are approximately conserved in the reactor experiments when the coupling interaction is turned off since the external stimulus $a(t)$ is still present acting on all reactors similarly to global coupling.

4.1. Outlook

We propose a small neural network with a similar architecture as the above reactor net using the Hodgkin–Huxley model as a suitable model for a single neuron to simulate the experimental observations of G. Laurent and coworkers. When a continuous stimulus (odor) is applied to all neurons and when the coupling term between a local neuron and the projection neurons is inhibitory, the projection neurons will fire coherently with a phase shift. The signatures (action potentials) of the projection neurons should approximately retain their appearance for coupled and uncoupled operation as required by experiment. This will be shown in further work.

Acknowledgements

We thank the Deutsche Forschungsgemeinschaft for financial support.

References

[1] D. Dechert, K.-P. Zeyer, F.W. Schneider, Recognition of phase patterns in a chemical reactor network, J. Phys. Chem. 100 (1996) 19043.
[2] W. Hohmann, M. Kraus, F.W. Schneider, Recognition in excitable chemical reactor networks. Experiment and model simulations, J. Phys. Chem. 101 (1997) 7364.
[3] W. Hohmann, M. Kraus, F.W. Schneider, Learning and recognition in excitable reactor networks, J. Phys. Chem. 102 (1998) 3103.
[4] W. Hohmann, M. Kraus, F.W. Schneider, Pattern recognition by electrical coupling of eight chemical reactors, J. Phys. Chem. A103 (1999) 7606.
[5] W. Hohmann, N. Schinor, M. Kraus, F.W. Schneider, Electrically coupled chemical oscillators and their action potentials, J. Phys. Chem. A103 (1999) 5742.
[6] K. MacLeod, G. Laurent, Distinct mechanisms for synchronization and temporal patterning of odor-encoding neural assemblies, Science 274 (1996) 976.
[7] M. Wehr, G. Laurent, Odour encoding by temporal sequences of firing in oscillating neural assemblies, Nature 384 (1996) 162.
[8] M. Stopfer, S. Bhagavan, B.H. Smith, G. Laurent, Impaired odour discrimination on desynchronization of odour-encoding neural assemblies, Nature 390 (1997) 70.
[9] K. MacLeod, A. Bäcker, G. Laurent, Who reads temporal information contained across synchronized and oscillatory spikes trains? Nature 395 (1998) 693.
[10] J.J. Hopfield, Pattern recognition computation using action potential timing for stimulus presentation, Nature 376 (1995) 33.
[11] W. Hohmann, J. Müller, F.W. Schneider, Phase shifting in a chemical oscillator to encode analogue information, J. Chem. Soc. Faraday Trans. 92 (1996) 2873.